동적 가황처리된 PP/EPDM 블렌드의 결정화 속도 연구: 베타 핵제의 효과

Bin Yang†, Yan-Li Deng, Xia Ru, Ji-Bin Miao, Ming Cao, Jia-Sheng Qian, Li-Fen Su, Peng Chen,
Jing-Wang Liu*, La-Xia Wu**, and Tao Pang**

College of Chemistry and Chemical Engineering, Institute of High Performance Rubber Materials & Products, and
Key Laboratory of Environment-Friendly Polymeric Materials of Anhui Province, Anhui University
*College of Polymer Science and Engineering, the State Key Laboratory of Polymer Materials Engineering, Sichuan University
**Collaborative Innovation Center for Petrochemical New Materials, Anqing Normal University
(2015년 12월 11일 접수, 2016년 3월 11일 수정, 2016년 4월 11일 채택)

Study on Crystallization Kinetics of Dynamically-Vulcanized PP/EPDM Blends: Effect of β Nucleating Agent

Bin Yang†, Yan-Li Deng, Xia Ru, Ji-Bin Miao, Ming Cao, Jia-Sheng Qian, Li-Fen Su, Peng Chen,
Jing-Wang Liu*, La-Xia Wu**, and Tao Pang**

College of Chemistry and Chemical Engineering, Institute of High Performance Rubber Materials & Products, and
Key Laboratory of Environment-Friendly Polymeric Materials of Anhui Province, Anhui University, Hefei, Anhui, P.R. China
*College of Polymer Science and Engineering, the State Key Laboratory of Polymer Materials Engineering,
Sichuan University, Chengdu, Sichuan, P.R. China
**Collaborative Innovation Center for Petrochemical New Materials, Anqing Normal University, Anqing, Anhui, P.R. China
(Received December 11, 2015; Revised March 11, 2016; Accepted April 11, 2016)

Abstract: Two types of β nucleating agents (β-NAs), aryl dicarboxylic acid amide (TMB-5) and diphenyl phthalate diamine (NT-C), were adopted to modify the polypropylene (PP)/ethylene propylene diene monomer (EPDM) blends, which were prepared by dynamic-vulcanization technology. Wide angle X-ray diffraction (WAXD) and differential scanning calorimetry (DSC) were used to study the crystallization kinetics of PP. Our results showed that the addition of β-NAs can considerably increase the crystallization temperature, and significantly decrease the spherulite size of β-PP (L_{300}). The Jeziorny analysis showed there were ~82% and ~89% of relative crystallinity generated from the primary crystallization in the composites containing TMB-5 and NT-C, respectively. The crystallization half time ($t_{0.5}$) showed that NT-C improved the overall crystallization rate more effectively than TMB-5. In addition, the peaks of the relative crystallization rate curves were shifted towards higher temperature by 14 and 9 °C with the addition of TMB-5 and NT-C, respectively.

Keywords: β nucleating agent, PP/EPDM, crystallization kinetics, toughening, dynamic-vulcanization.

Introduction

Polypropylene (PP) is a polymorphic material with several crystal modifications including monoclinic (α), hexagonal (β), and orthorhombic (γ) forms, etc. As compared with α phase, β-form crystal has higher impact strength and heat deformation temperature (HDT).[1-3] Till now, PP has gained wide application in many fields due to its excellent chemical properties, processability as well as well mechanical strength. However, the low impact resistance of PP (especially at low temperature) still seriously limits its further promotion and wider applications.[4-8] In an attempt to improve the impact toughness of PP, PP/ethylene-propylene-diene monomer (EPDM) thermoplastic vulcanizates (TPVs) have been widely used.[9-12] Chakraborty et al.[9] reported the great improvement in elongation at break and impact performance of the PP/EPDM TPVs after the use of phase modifiers. Nevertheless, the rubber toughening strategy usually sacrifices the modulus and strength of PP.[13-15]

Lots of research work had been done to improve the toughness of PP materials with limited loss in rigidity and strength through introducing the β nucleating agent (β-NA) into TPVs. Tang et al.[16] studied the effect of β phase on the fracture behavior of the PP/EPDM/β-NA composites using the specific essential work of fracture (w_e). They observed that when the β-crystal content was 42.2%, there was an increase in the value of w_e by 52%. Ma et al.[17] found that the impact strength of the PP/EPDM/β-NA composites with 0.5 wt% of β-NA loading was 10 times more than that of neat PP, and a synergic toughening mechanism between rubber and β-NA for the composites was also proposed in their study.

As is well known, the properties of composites containing crystallizable component usually depend largely on the extent of crystallinity and the crystallization behavior of the crystallizable one.[18,19]

To the date, there are still limited studies on the effect of the β-NA on the crystallization kinetics of PP in PP/EPDM blends. Wide angle X-ray diffraction (WAXD) and differential scanning calorimetry (DSC) were employed to investigate the inducing effect of β-NA on the formation of β-PP and crystallization kinetics of PP in PP/v-EPDM composites. Our findings showed that the relative content of β phase ($K_β$) was about 90% in the PP/v-EPDM/TMB-5 composites. As the NT-C content increased, $K_β$ first increased and then decreased with a largest value of 82% with a 0.6% loading of NT-C. The addition of β-NAs could largely enhance the crystallization temperature, and decrease the spherulite size of β-PP (L_{300}), which decreased with the increase of $K_β$. In addition, the crystallization half time ($t_{0.5}$) showed that NT-C improved the overall crystallization rate more effectively than TMB-5. The present work provides a better understanding of the crystallization characteristics of PP, which will be helpful to further studies on the optimization of processing parameters of PP in industrial applications.

Experimental

Materials. Ethylene-propylene-diene monomer (EPDM, model: 4785-HM) in this study was supplied by Dow Chemical Co., U.S.A., containing 68 wt% of ethylene and 27 wt% of propylene, respectively. Polypropylene (PP, model: T30S) used was obtained from Lanzhou Petrochemical Co., China, with a melt flow rate (MFR) of 2.8 g/10 min (under 2.16 kg/230 °C) and a density of 0.91 g/cm³. Besides, two nucleating agents (denoted as β-NA-1 and β-NA-2) were TMB-5 and NT-C,

respectively, which were both obtained from Jingsichen Industry & Trade Co., China. In addition, peroxide cumene (DCP) from Hengnuo Chemical Co., Ltd.; zinc oxide, HG 3623-99, from Hongyan Chemical Reagent Co., Ltd; and antioxidant 1010 (AT-10), from Shengnuo Plastic Material Co., were used as received.

Sample Preparation. The melt reactive blending process for preparing TPV samples (PP/EDPM=80/20 in weight percent) was carried out in a HAAKE torque rheometer with a screw speed of 60 rpm at 180 °C for 7 min. The β-NA contents were 0, 0.2, 0.4, 0.6 and 0.8 wt% (to the total weight of the blends). The PP, EPDM, β-NA and vulcanizing agents (DCP, AT-10, zinc oxide) were simply mixed at first, and then added to the HAAKE torque rheometer. The resultant mixture was mixed on an open mill at 170 °C for 15 min. Finally, the composites were molded as a sheet on a hot press at 180 °C for 10 min. Neat PP and PP/EPDM blend without β-NA or vulcanizing agent were prepared for comparative study. The obtained composites were cut into standard samples for further characterizations. In this work, neat PP and PP/EPDM blends without vulcanizing agents were also designated as TPV(s), with the crosslinking degree of zero. For brevity, TPVs with different β-NA dosages were designated as follows: PP/v-EPDM (0 wt%), β-NA 0.2 (0.2 wt%), β-NA 0.4 (0.4 wt%), β-NA 0.6 (0.6 wt%) and β-NA 0.8 (0.8 wt%), respectively.

Characterizations. Differential Scanning Calorimetry (DSC) Measurement: The non-isothermal crystallization behavior was investigated on a Perkin-Elmer differential scanning calorimeter (DSC), model: DSC-2C. In the tests, samples of about 3~5 mg were scanned from 30 to 200 °C at a heating rate of 10 °C/min in a nitrogen (N_2) atmosphere, and kept at 200 °C for 5 min for removal of thermal history. Afterwards, the samples were cooled to 30 °C at 10 °C/min. An empty aluminum pan served as a reference. The absolute crystallinity (X_c) of samples was calculated from the follow eq. (1):

$$X_c = \Delta H_c/(\varphi_1 \times \Delta H_0) \times 100\% \tag{1}$$

where ΔH_c was the enthalpy of fusion of samples as obtained by DSC, φ_1 the mass fraction of PP in the blends/composites, and ΔH_0 the enthalpy of fusion for 100% crystalline polymer which was taken as 209.0 J/g for PP in this study.[20]

Wide Angle X-ray Diffraction (WAXD): WAXD measurements were carried out using a XD-3 X-ray diffractometer (Puxi General Instrument Co., Ltd., P.R. China) at the room temperature at an accelerating voltage of 36 kV with the Cu-

Kα (λ=1.541 nm) as radiation source. The WAXD patterns were collected by monitoring the diffractions with the 2θ ranging from 5° to 40° at a scanning speed of 4°/min.

Results and Discussion

Non-isothermal Crystallization and Melting Behaviors. Figure 1(a) and 1(b) showed the melting behaviors of TPVs. There was one melting peak at about 163 °C on the melting curves of PP, PP/EPDM and PP/v-EPDM, which belonged to the endothermic peak of α phase of PP. However, as for the samples with β-NA, there existed two melting peaks in the melting curves at 142 and 163 °C corresponding to the characteristic peaks of β and α phases of PP, respectively.[21] The peak melting temperatures of PP/EPDM and PP/v-EPDM were both lower than that of neat PP. This could be because the presence of EPDM affected the movement and rearrangement of the PP molecular chains, leading to the imperfect crystals.[17,22]

In Figure 1(b), for NT-C 0.2%, the endothermic peak of β phase did not appear when the β-NA content was low; while the melting peaks of β-PP can be clearly seen for NT-C 0.4%, NT-C 0.6% and NT-C 0.8%. Besides, a small peak appeared at the high temperature side of the melting peak of β-PP, which could be attributed to the recrystallization of β-PP.[16] It should be noted that the peak melting temperatures of α phase were shifted to the higher value with increasing β-NA content, indicating a higher degree of crystal perfection for α-PP.

The crystallization behaviors of the TPVs were showed in Figure 1(c) and 1(d). It was observed that the crystallization peak temperature of neat PP was 113.0 °C. However, the addition of β-NA into PP caused an obvious shift of the crystallization peak towards higher temperature. With the addition of TMB-5, the crystallization peak temperature of the composites was shifted from 113 to 127 °C. The addition of NT-C increased the crystallization peak temperature of PP by 9 °C. The β-NA had good nucleating effect, causing PP to crystallize
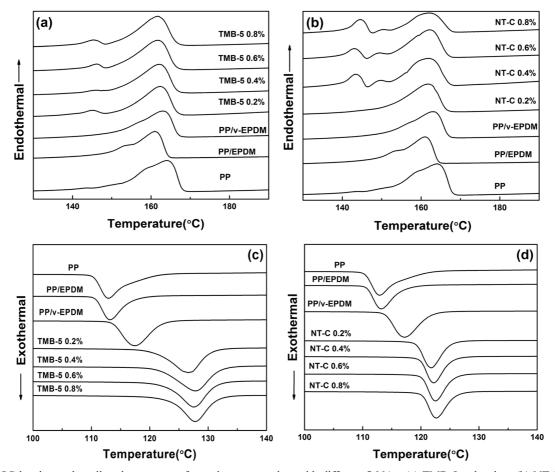

Figure 1. DSC heating and cooling thermograms for various composites with different β-NAs: (a) TMB-5 at heating; (b) NT-C at heating; (c) TMB-5 at cooling; (d) NT-C at cooling.
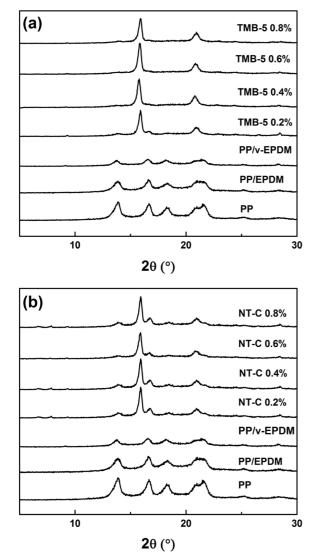
Figure 2. X-ray diffraction curves for various composites with different β-NAs: (a) TMB-5; (b) NT-C.

Table 1. Crystal-related Parameters for the Samples Containing Different Contents of β-NA

Sample	L_{300} (nm)	K_β (%)	X_c (%)
PP	-	-	44.17
PP/EPDM	38.89	0.04	35.09
PP/v-EPDM	19.45	0.09	33.02
TMB-5 0.2%	5.56	0.89	39.02
TMB-5 0.4%	4.62	0.92	39.47
TMB-5 0.6%	5.19	0.91	38.05
TMB-5 0.8%	5.19	0.90	39.94
NT-C 0.2%	5.19	0.74	43.17
NT-C 0.4%	5.19	0.74	44.73
NT-C 0.6%	4.09	0.82	43.85
NT-C 0.8%	5.19	0.74	44.16

the β-PP crystal. Meanwhile, the α diffractions almost disappeared, indicating that the addition of β-NA depressed the growth of α crystal and resulted in the transformation from α-type to β-type crystals, which was in accordance with previous literature.[17] The value of K_β,[21] the relative content of β phase, was evaluated from the WAXD diffractograms as below eq. (2):

$$K_\beta = \frac{I_\beta}{I_{\alpha 1}+I_{\alpha 2}+I_{\alpha 3}+I_\beta} \times 100\% \qquad (2)$$

where I_β was the intensity of the (300) reflection of the β phase, and $I_{\alpha 1}$, $I_{\alpha 2}$ and $I_{\alpha 3}$ the intensities of (110), (040) and (130) reflections of the α phase, respectively. The kinetic parameters of crystallization can be obtained from DSC and WAXD, as listed in Table 1. The crystallite sizes L_{hkl} in the direction perpendicular to (hkl) planes were estimated by using Scherrer equation,[16] eq. (3):

$$L_{hkl} = k/(B \cdot \cos\theta) \qquad (3)$$

where 2θ was the diffraction angle, B the reflection breadth at half-maximum and k the X-ray wavelength. For the determination of the crystallite size, the crystalline reflection (300) of the β phase was selected. The crystallite size L_{300} became smaller when adding β-NA. It is well known that fine spherulites could usually overcome the defects originating from the stress concentration in the products, leading to good toughening effect.[25] With the addition of 0.4% TMB-5 and 0.6% NT-C, the crystallite sizes of β phase, L_{300}, reached their minimum values of 4.62 and 4.09 nm, respectively. At the same

at higher temperature during the melt cooling process.[23]

Crystalline Structures. To verify the crystalline structures, WAXD measurements were employed and the results were shown in Figure 2. The WAXD patterns of neat PP displayed five distinct peaks at 2θ=14.1°, 16.9°, 18.5°, 21.2° and 21.9°, which corresponded to the (110), (040), (130), (131) and (111) reflections of α phase, respectively.[24] As can be seen, the height of diffraction peaks of α phase decreased after introducing EPDM. The presence of EPDM was speculated to constrain the molecular chains' movement and diffusion during the crystal growth to some extent, resulting in the formation of imperfect crystals. When adding the β-NA, a strong peak appeared at 2θ=16.0° corresponding to the (300) reflection of

time, their K_β values also achieved the maximum. Here, spatial confinement provided a good explanation for the development of β-PP. Interestingly, the K_β value was high, but the endothermic peak of the β phase in DSC seemed quite small. Actually, the determination of the exact β content was difficult using DSC method since there existed the transformation from β-crystals to α-crystals during the heating process.[22] It should also be noted that the absolute crystallinity (X_c) almost remained unchanged with increasing β-NA content. The samples containing NT-C bore higher crystallinity values than those containing TMB-5, suggesting that NT-C provided more nucleation sites for PP than TMB-5.

Jeziorny Analysis. The Avrami equation has been widely used to analyze the kinetics of polymer isothermal crystallization, eq. (4),

$$X_t = 1 - \exp(-Z_t \cdot t^n) \tag{4}$$

where Z_t was the crystallization rate constant describing the nucleation and growth rate and n the Avrami exponent relating to the mechanism of nucleation as well as the growth method of crystal. During a non-isothermal crystallization process, the cooling rate ϕ should also be taken into consideration, and the parameter Z_t should accordingly be corrected as suggested by Jeziorny.[26] At a cooling rate of ϕ, the modified form of the rate constant (Z_c) for the non-isothermal crystallization was expressed as eq. (5),

$$\log Z_c = \log Z_t / \phi \tag{5}$$

The plots of $\log[-\ln(1-X_t)]$ *versus* $\log t$ for all the samples were shown in Figure 3. All plots comprised two distinct regions corresponding to the primary and secondary crystallizations, respectively. Both crystallization stages can be linearly correlated. It was seen that there existed a turning point for two crystallization stages on each curve, as indicated by the dot line. The turning point occurred at a constant crystallinity X_t of ~82% and ~89% for samples with TMB-5 and NT-C, respectively, regardless of the β-NA content.

The values of n_1, n_2, Z_{c1} and Z_{c2} were summarized in Table 2, with the subscripts 1 and 2 denoting the primary and secondary crystallization, respectively. It was observed that the addition of β-NA increased the value of n_1 from 5.2 to 7.9. The changes of n_1 value showed that β-NA increased the crystal growth rate of PP in the composites. The values of n_1 of all samples were greater than 3, which indicated that the crys-
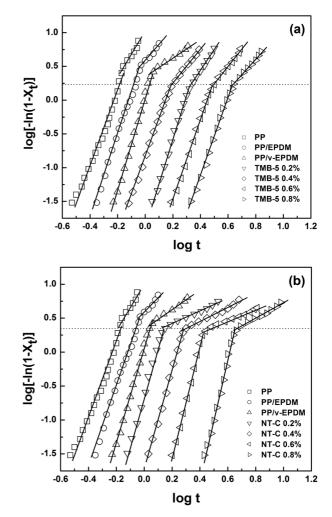

Figure 3. Plots of $\log[-\ln(1-X_t)]$ *versus* $\log t$ for various composites with different β-NAs: (a) TMB-5; (b) NT-C.

Table 2. Summary of Jeziorny Parameters of the Samples Containing Different Contents of β-NA

Sample	Primary		Secondary	
	n_1	Z_{c1}	n_2	Z_{c2}
PP	5.2	0.76	2.5	0.95
PP/EPDM	6.8	0.77	1.6	1.03
PP/v-EPDM	6.0	0.84	1.8	1.03
TMB-5 0.2%	6.8	0.78	2.8	0.91
TMB-5 0.4%	5.5	0.82	2.2	0.97
TMB-5 0.6%	6.3	0.81	2.6	0.94
TMB-5 0.8%	6.0	0.82	2.1	0.97
NT-C 0.2%	7.5	0.87	1.0	1.05
NT-C 0.4%	7.5	0.87	1.0	1.05
NT-C 0.6%	7.8	0.80	0.8	1.05
NT-C 0.8%	7.9	0.78	1.0	1.04

tallization was governed by three-dimensional growth.[27] In the secondary crystallization stage, the values of n_2 were less than that of n_1 in the same TPVs, indicating that the crystal dimension decreased. the Avrami exponent n_2 values of TPVs with TMB-5 were between 2.1 and 2.8, suggesting the growth of PP in composites primarily occurred in two- or three-dimensional mechanism. While n_2 values of TPVs with NT-C were between 0.8 and 1.0, the grown spherulite had occupied most of the space of samples in primary crystallization, and the rest of space was not enough to complete the rest of the spherulite growth during secondary crystallization.[28]

The Jeziorny rate parameter Z_c described the nucleation and growth rate. The larger the Z_c, the higher the crystallization rate. From the Z_c values listed in Table 2, it was obvious that the variations of Z_c value were among 0.78-0.82 and 0.78-0.87 for the TMB-5 TPVs and NT-C TPVs, respectively. All Z_c values of the composite materials were larger than that of neat PP, indicating that both EPDM and β-NA could be favorable to PP from the viewpoint of the crystallization rate.

Kinetics of Non-isothermal Melt Crystallization. The relative degree of crystallinity, X_t, was defined as below eq. (6):

$$X_t = X(t)/X(\infty) = \frac{\int_{T_o}^{T} (dHc/dT)dT}{\int_{T_o}^{T\infty} (dHc/dT)dT} \tag{6}$$

Where T_o and T_∞ are the onset and end crystallization temperatures, respectively.[29] The relationship between relative crystallinity (X_t) and temperature was shown in Figure 4. All curves displayed a typical sigmoidal shape, indicating that the crystallization process of polymers consisted of three sections: (1) the crystallization induction period, when X_t almost remained unchanged; (2) the primary crystallization period, when X_t increased sharply with the elapsed time; (3) the post-crystallization stage, when X_t gradually reached its maximum value until achieving 100% crystallinity. As can be seen, the crystallization temperature increased with increasing β-NA content, suggesting that the existence of β-NA played a good role in increasing the probability of the contact between chain segments and crystal nucleus. Hence, the composites could reach higher crystallinity at elevated temperatures.[30]

Under the same thermal history, the X_t vs. time plots (Figure 5) can be obtained using the following eq. (7),

$$t = (T_0 - T)/\phi \tag{7}$$

where T was the temperature at crystallization time t and ϕ the
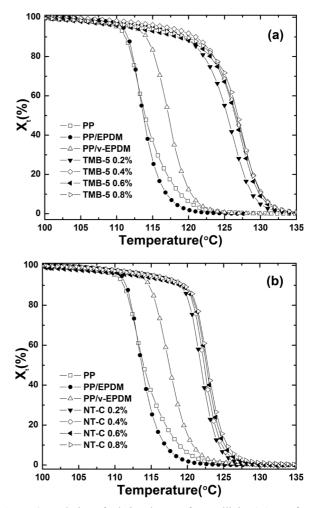

Figure 4. Evolution of relative degree of crystallinity (X_t) as a function of crystallization temperature for various composites with different β-NAs: (a) TMB-5; (b) NT-C.

cooling rate.[31] It was found in Figure 5 that the X_t of TPVs containing TMB-5 increased much slower than PP/EPDM and PP/v-EPDM, and the times of complete crystallization of TPVs containing TMB-5 were longer than those containing NT-C. This can also be seen from two time-related parameters, the crystallization half time ($t_{0.5}$) and the crystallization induction time (t_i), which were listed in Table 3. The parameters $t_{0.5}$ and t_i were the measure of the overall crystallization rate (OCR) and the nucleation rate, respectively. The smaller the value of t_i, the faster the nucleation rate. Higher nucleation rate always existed with more effective β-NA, thus promoting the OCR (indicative of the reduced $t_{0.5}$ value).[32] From Table 3, it was found that the incorporation of β-NA into TPVs significantly decreased both $t_{1/2}$ and t_i. For the sample with 0.4 wt% NT-C, the value of t_i decreased from 1.87 to 0.92 min in comparison
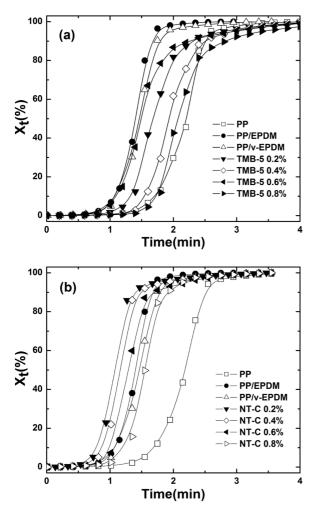
Figure 5. Evolution of relative degree of crystallinity (X_t) as a function of crystallization time (t) for various composites with different β-NAs: (a) TMB-5; (b) NT-C.

Table 3. Crystallization Times of the Samples Containing Different Contents of β-NA

Sample	t_i (min)	$t_{0.5}$ (min)
PP	1.87	2.20
PP/EPDM	1.23	1.65
PP/v-EPDM	1.20	1.38
TMB-5 0.2%	1.25	1.68
TMB-5 0.4%	1.55	1.93
TMB-5 0.6%	1.08	1.46
TMB-5 0.8%	1.72	2.08
NT-C 0.2%	0.93	1.16
NT-C 0.4%	0.92	1.15
NT-C 0.6%	1.09	1.31
NT-C 0.8%	1.31	1.56

to neat PP, indicating that the nucleation rate of PP was remarkably enhanced in presence of NT-C.

Relative Crystallization Rate (RCR). Figure 6 showed the variation of relative crystallization rate (RCR), i.e., (dX_t/dt), as a function of the crystallization temperature. As it is known, the rates of the crystal nucleation and crystal growth are both dependent on the temperature. The RCR also reflects the overall rate of crystallization, a combination of both nucleation and growth stages. When the temperature is lower than the melting temperature, the thermodynamic factors with lowest and most stable energy induce the crystallization of macromolecular chains, the lower temperature (or high cooling rate) will be more favorable for polymer crystal growth.[26,33] From the Figure 6, it was observed that the addition of EPDM enhanced the (dX_t/dt)$_{max}$ of PP from 1.7 to 2.2 s^{-1}, but hardly showed any effect on the onset crystallization temperature (T_o). The addi-
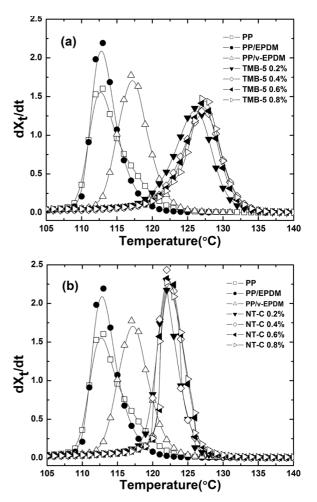

Figure 6. Variation of relative crystallization rate (dX_t/dt) as a function of crystallization temperature for various composites with different β-NAs: (a) TMB-5; (b) NT-C.

tion of the curing agents, however, caused an obvious decrease of $(dX_t/dt)_{max}$ to 1.8 s^{-1}, since the vulcanized EPDM structures presented more chain entanglement and the steric hindrance, which slowed down the crystal growth rate and thus lowered the crystallization rate.[34,35] Besides, the peaks of crystallization rate curves were found to be shifted towards high temperature by 14 °C with the addition of TMB-5 (in accordance with our earlier discussion in Figure 1 and 4), suggesting that TMB-5 played a good role in increasing the probability of the contact between crystal nucleus and chain segments.[29] Additionally, it can be seen that the relative crystallization rate (RCR) displayed a progressively rising trend with the addition of NT-C. RCR had a maximum value of 2.4 s^{-1} at NT-C%=0.4%. While the $(dX_t/dt)_{max}$ of TPVs containing TMB-5 was 1.5 s^{-1}, which indicated that NT-C provided more nucleation sites, leading to an enhanced nucleation rate.

Conclusions

In this study, two kinds of β-NAs (TMB-5, NT- C) were employed to prepare the PP/EPDM/β-NA composites. The effect of β-NA on formation of β crystals and crystallization kinetics of PP in the composites were studied by WAXD and DSC. Our findings showed that the K_{β} was about 90% in PP/v-EPDM/TMB-5 composites and the content of TMB-5 had little effect on it. With the increase of NT-C content, K_{β} first increased and then decreased with a maximum value of 82% when NT-C% was 0.6%. The crystallite size L_{300} decreased with increasing K_{β}. It can be seen that all curves in Figure 4 and 5 had similar sigmoidal shape, indicating the existence of nucleation, primary and secondary crystallizations. There existed turning points on the Jeziorny plots at nearly constant X_t of ~82% and ~89% for samples with TMB-5 and NT-C, respectively. From the RCR curves, it was found that the peaks were shifted towards high temperature by 14 and 9 °C with the addition of TMB-5 and NT-C, respectively. Additionally, the crystallization half time ($t_{0.5}$) value showed that NT-C improved the overall crystallization rate (OCR) more effectively than TMB-5. The present work could supply a better understanding of the crystallization characteristics of PP materials, and give an insight into further research on the design of PP composites with desirable crystalline structures.

References

1. J. Lee, H. Kim, and H. J. Kang, *Polym. Korea*, **36**, 803 (2012).
2. N. Zhang, Q. Zhang, and K. Wang, *J. Therm. Anal. Calorim.*, **107**, 733 (2012).
3. G. Liu, *Polym. Korea*, **39**, 268 (2015).
4. M. Lazaar, S. Bouadila, S. Kooli, and A. Farhat, *Appl. Therm. Eng.*, **68**, 62 (2014).
5. X. G. Tang, B. Yang, and M. B. Yang, *Colloid Polym. Sci.*, **287**, 1237 (2009).
6. A. R. Dickson, D. Even, J. M. Warnes, and A. Fernyhough, *Composites Part A*, **61**, 258 (2014).
7. S. W. Lee, W. Huh, U. Hyun, D. H. Lee, and S. K. Noh, *Polym. Korea*, **27**, 509, (2003).
8. C. G. Wang, Z. S. Zhang, and K. C. Mai, *J. Therm. Anal. Calorim.*, **106**, 895 (2011).
9. M. Khodabandelou, M. K. R. Aghjeh, and M. Mazidi, *Rsc. Advances*, **5**, 70817 (2015).
10. P. Chakraborty, A. Ganguly, S. Mitra, and A. K. Bhowmick, *Polym. Eng. Sci.*, **48**, 477 (2008).
11. Y. K. Chen, C. H. Xu, and Y. P. Wang, *Polym. Eng. Sci.*, **53**, 27 (2013).
12. S. Dubinin, Z. Hrdlicka, J. Simek, A. Kuta, and V. Duchacek, *Kautsch. Gummi. Kunstst*, **68**, 67 (2015).
13. A. Thompson, Q. Bianchi, C. L. G. Amorim, and G. Machado, *Polymer*, **52**, 1037 (2011).
14. K. H. Yoon, D. Y. Shin, and Y. C. Kim, *Polym. Korea*, **36**, 245 (2012).
15. A. F. Jolfaei, J. N. Gavgani, A. Jalali, and F. Goharpey, *Polym. Bull.*, **72**, 1127 (2015).
16. X. G. Tang, R.Y. Bao, and W. Yang, *Eur. Polym. J.*, **45**, 1448 (2009).
17. L. F. Ma, W. K. Wang, and R. Y. Bao, *Mater. Des.*, **51**, 536 (2013).
18. H. G. Wu, N. Y. Ning, and L. Q. Zhang, *J. Polym. Res.*, **20**, 266 (2013).
19. E. K. Jurgen, P. A. Schawe, and M. D. Vermeulen, *Colloid Polym. Sci.*, **293**, 1607 (2015).
20. D. M. Stelescu, A. Airinei, M. Homocianu, N. Fifere, D. Timpu, and M. Aflori, *Polym. Test.*, **32**, 187 (2013).
21. X. G. Tang, W. Yang, and R. Y. Bao, *Polymer*, **50**, 4122 (2009).
22. Q. F. Yi, X. J. Wen, and J. Y. Dong, *Polymer*, **49**, 5053 (2008).
23. D. Ponnamma, J. George, and M. G. Thomas, *Polym. Eng. Sci.*, 55, 1203 (2015).
24. N. Y. Ning, Q. J. Yin, and F. Luo, *Polymer*, **48**, 7374 (2007).

25. D. P. Huang, L. Li, and J. Hu, *Modern Plast. Proc. Appl.*, **20**, 38 (2008).

26. B.Yang, M. B. Yang, and W. J. Wang, *Polym. Eng. Sci.*, **52**, 21 (2012).

27. U. Nattapon, J. Methakarn, P. Zheng, J. Banja, N. Charoen, and T. Anoma, *Polym. Test.*, **44**, 101 (2015).

28. B. Yang, L. Hu, R. Xia, and F. Chen, *Macromol. Res.*, **24**, 74 (2016).

29. G. T. Liu, J. Lei, and F. Y. Wang, *Polym. Eng. Sci.*, **53**, 2535 (2013).

30. Y. J. Tao, Y. X. Pan, and K. C. Mai, *Eur. Polym. J.*, **44**, 1165 (2008).

31. B.Yang, J. Z. Lin, and R. Xia, *J. Macromol. Sci. Phys.*, **53**, 462 (2014).

32. C. H. Xu, X. D. Cao, and X. J. Jiang, *Polym. Test.*, **32**, 507 (2013).

33. P. S. He, *Int. Polym. Proc.*, **30**, 217 (2012).

34. Y. Zare and H. J. Garmabi, *Appl. Polym. Sci.*, **214**, 1225 (2012).

35. H. Liu and H. Huo, *Colloid Polym. Sci.*, **292**, 849 (2014).